GEOPHYSICAL RESEARCH LETTERS, VOL. 24, NO.11, PAGES 1427-1430, JUNE 1, 1997

Evidence of currents and unstable particle distributions in an extended region around the lunar plasma wake

S. D. Bale[1], C. J. Owen[1], J.-L. Bougeret[2], K. Goetz[3], P. J. Kellogg[3], R. P. Lepping[4], R. Manning[2], S. J. Monson[3]

Abstract. We report observations of electrostatic ion acoustic waves and Langmuir waves during a recent lunar encounter by the Wind spacecraft. These waves are observed when Wind is magnetically connected to the nominal wake and at distances greater than 8 lunar radii from the wake. When interpreted in the context of a simple time-of-flight model, these observations imply the existence of a system of currents and disturbed particle distributions that extends far into solar wind.

Introduction

It has long been known that a depleted plasma wake forms behind the moon [*Schubert and Lichtenstein*, 1974]. Lacking an internal magnetic field, and hence bow shock, solar wind particles impact the lunar surface and are absorbed and removed from the particle distribution functions. A guiding center model of the solar wind ion population [*Whang*, 1968] does well to explain the observed plasma depletion [*Lyon et al.* 1967; *Ogilvie et al.* 1996; *Bosqued et al.*, 1996] antisunward of the moon. However, it has always been assumed that the solar wind electrons are merely Boltzmann in this interaction. On December 27, 1994, as part of an orbital manuever sequence, the Wind spacecraft came within 6.8 R_l of the moon and was eclipsed in the lunar umbra for roughly 41 minutes. A special issue of *Geophysical Research Letters* (Volume 23, Number 10, 1996) contains several papers reporting lunar wake observations. In this letter, we provide further observations of plasma waves and demonstrate that these are strongly correlated with intervals when the spacecraft is magnetically connected to the moon/wake system. We suggest that this is evidence of an extended region of currents and unstable particle distributions around the lunar wake.

Wind Observations

Plasma wave observations in and near the lunar wake on December 27, 1994 reveal several distinct features [viz., *Kellogg et al.* 1996; *Farrell et al.*, 1996].

[1]Astronomy Unit, Queen Mary and Westfield College, London
[2]DESPA, Observatoire de Paris, Meudon
[3]School of Physics and Astronomy, University of Minnesota
[4]NASA Goddard Space Flight Center

Paper number 97GL01193.
0094-8534/97/97GL-01193$05.00

To understand these observations, we use magnetic field measurements from the Wind magnetometer [*Lepping et al.* 1995], corrected for spin phase error in eclipse [*Owen et al.*, 1996], to transform to the selenocentric coordinate system shown in Figure 1 . The system is defined as having $\hat{Z}_{LC} = \hat{X}_{GSE} \times \hat{B}_{GSE}$ and $\hat{X}_{LC} = -\hat{X}_{GSE}$ with $\hat{Y}_{LC}$ completing a right-handed system. For each magnetic field vector, the system is rotated about the $\hat{X}_{GSE}$ axis such that the $\hat{Z}_{LC}$ component of the magnetic field vanishes; the magnetic field vector then lies in the meridian plane. The position of the spacecraft with respect to the moon is then computed. We have assumed implicitly that the direction of the solar wind flow is $-X_{GSE}$; this is accurate to 2.5 degrees [*Ogilvie et al.*, 1996].

Since $B_z = 0$ in the new frame, the geometry is reduced to a two dimensional slab. In this system, the spacecraft is connected to the moon and/or wake whenever the spacecraft elevation $|Z_{sc}| \leq 1$ (in lunar radii) and when the IMF intersects the wake at $X_{wake} \geq -1/\sin\phi$, where $\phi = \tan^{-1}(B_y/B_x)$.

Figure 2 shows the WAVES observations and the two parameters X_{wake} and Z_{sc}. The top panel shows observations from the Thermal Noise Receiver (TNR) [*Bougeret et al.* 1995] and the second panel shows FFT receiver observations, both are electric field spectrograms measured on the 100 m tip-to-tip spin plane antenna. The FFT measurements (panel (b)) have been averaged over 1 minute; missing spectra due to instrument mode changes are evident throughout the interval. Panels (c) and (d) show X_{wake} and Z_{sc}, respectively, as described above and the dark vertical band corresponds to the optical shadow. The dotted line at $X = -1/\sin\phi$ in panel (c) marks the lower boundary of magnetic connection to the moon/wake system. The horizontal band in panel (d) gives the condition $|Z_{sc}| \leq 1$ for magnetic connection.

The broadband, ion acoustic component, peaked near 5 kHz, is first observed at 12:30 UT in panel (b). At this time, Wind was roughly 8 R_l from the moon ($1R_l$ = 1738 km) and about 7 R_l from the edge of the wake structure. The waves persist until 17:00 UT, roughly 1.5 hours and 6 R_l after exiting the wake, and then cut off abruptly. Due to the large distance from the wake and the electrostatic nature of the waves, it was originally assumed [*Kellogg et al.*, 1996] that the waves were not directly related to the wake.

It is clear from Figure 2 that the waves are observed when Wind is magnetically connected, or nearly so, to

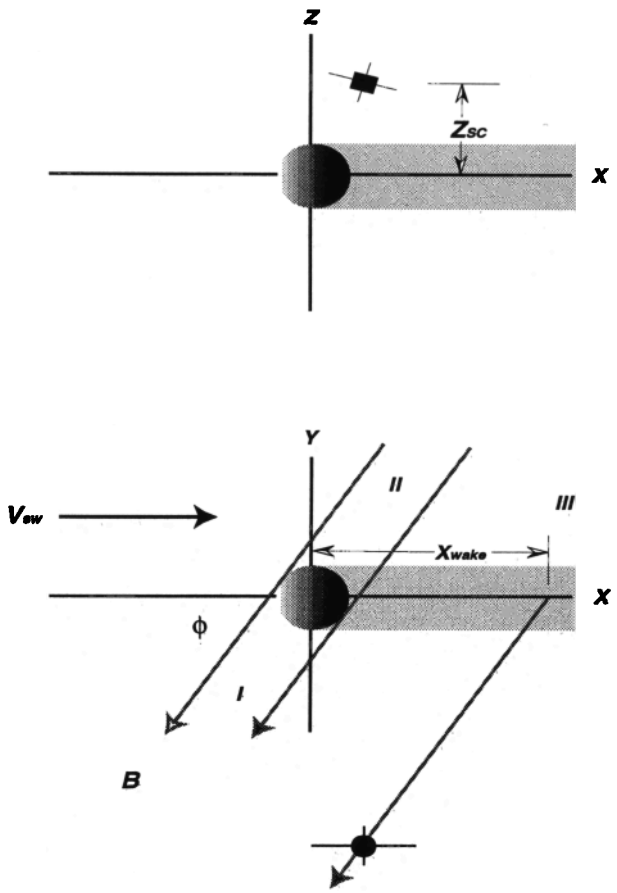

Figure 1. We transform spacecraft position at each $\vec{B}$-field measurement to a selenocentric frame with $\hat{Z}_{LC} = \hat{X}_{GSE} \times \hat{B}_{GSE}$ and $\hat{X}_{LC} = -\hat{X}_{GSE}$ with $\hat{Y}_{LC}$ completing a right-handed system. We also calculate X_{wake}, the $\hat{X}$ coordinate of the point of intersection of the spacecraft flux tube with $Y' = 0$. In this frame, the spacecraft is magnetically connected to the lunar plasma wake whenever $|Z_{sc}| \leq 1$ and $X_{wake} > -1/\sin(\phi)$.

the nominal wake or the moon itself. The FFT Receiver (panel (b)) observes a good correlation between bursts of broadband ion acoustic waves and intervals in which $|Z_{sc}| \leq 1$. Data from the magnetic channels of the FFT show no response at these frequencies, confirming that the waves are electrostatic. At just around 13:30 UT, X_{wake} is roughly 15 R_l; this is largest value of X_{wake} showing acoustic noise during this encounter. At 14:15 UT, the parameter X_{wake} drops by roughly 5 R_l; here, the IMF maps to a region of the wake which is closer to the moon and the corresponding wave amplitudes are larger. The ion acoustic noise persist until 17:00 UT when Wind leaves the connection slab.

Langmuir waves (Figure 2a) were observed near the local plasma frequency following the depleted density profile through the ion wake region. These are similar to the Langmuir waves often observed near the solar wind-electron foreshock boundary [*Filbert and Kellogg*, 1979] on field lines magnetically connected to the bow shock. During these events, however, Wind is nearly $50R_e$ upstream of that boundary. A similar observation was made near the moon with the RAE-2 satellite [*Weber et al.*, 1976]. The TNR receiver observations show a similar correlation between magnetic connection and wave activity. Noise enhancements at 17 kHz begin at 12:15 UT when Wind is just near the connection slab ($Z_{sc} \approx 1$). After passing through the wake, Wind is magnetically connected closer to the moon and the intensity of the waves is larger. The burst of Langmuir waves between 15:45-16:00 UT shows some evidence of frequency downshift; this is characteristic of the 'beam mode' branch of the Langmuir wave dispersion relation [*Fuselier et al.*, 1985; *Cairns* 1989] and indicates an effective beam speed that is of the order of the electron thermal speed. Just before 17:00 UT, the Langmuir waves cut off abruptly as Wind leaves the

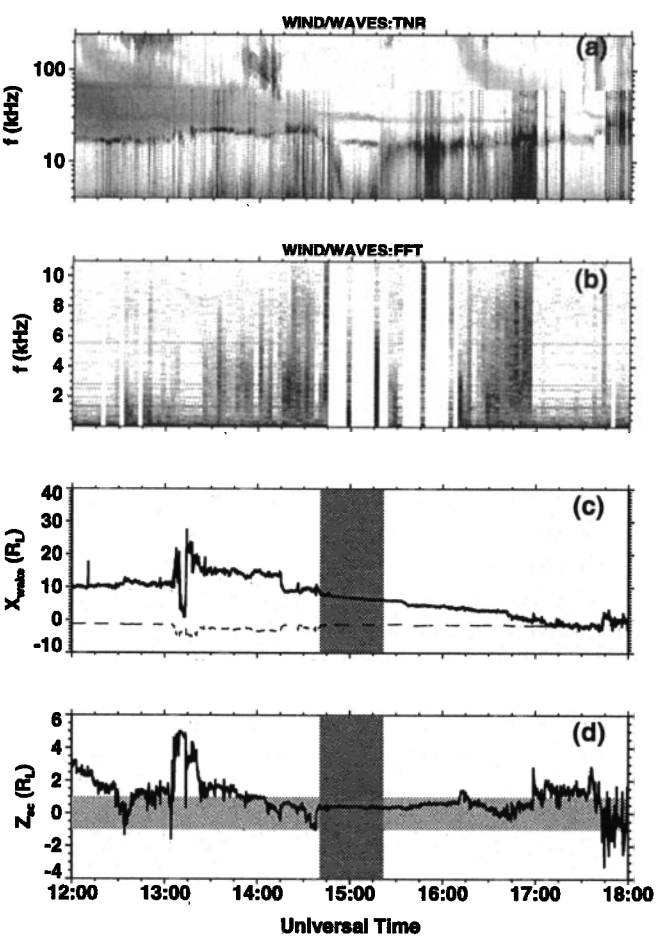

Figure 2. Plasma wave measurements show broadband ion acoustic noise (panel b) and Langmuir and beam mode waves (panel a) when the spacecraft is magnetically connected to the moon/wake system. When the spacecraft elevation is within 1 lunar radius of the origin ($|Z_{sc}| \leq 1$), and the IMF intersects the wake ($X_{wake} \geq -1/\sin\phi$), the spacecraft is magnetically connected. The dotted line in panel (c) is the lower bound $X = -1/\sin\phi$ for magnetic connection. The vertical bands show the time of optical shadow. The broadband ion acoustic noise in panel (b) is evidence of neutralizing electric currents.

connection slab. Between 17:45 and 18:00 UT, there is an intense burst of Langmuir waves near the local plasma frequency. The parameter X_{wake} is fluctuating around -1; this implies that the local magnetic field line is connected to the moon itself.

A Guiding Center Description

At any point downstream of the magnetic tangent line to the moon, the particle velocity distributions will be modified; particles whose guiding-center trajectories take them through the moon will be absorbed and removed from the distribution. *Whang* [1968] used a guiding-center model to describe the ion void observed by Explorer 35. In this model, the field aligned velocity distribution is Maxwellian, $f(v) = \frac{n_0}{\pi^{1/2} v_{th}} e^{-v^2/v_{th}^2}$ in the solar wind rest frame, where $v_{th} = \sqrt{2k_b T/m}$ is the thermal speed; there is only Larmor gyration in the perpendicular directions. Using the geometry of Figure 1, one can calculate [*Whang*, 1968] two cutoff velocities within which the solar wind particles are absent. These cutoffs speeds are defined as

$$\gamma_1 = v_1/v_{sw} = \sin(\alpha + \lambda)/\sin(\phi - \alpha - \lambda) \quad (1)$$

$$\gamma_2 = v_2/v_{sw} = \sin(\alpha - \lambda)/\sin(\phi + \alpha - \lambda) \quad (2)$$

where $\lambda = \tan^{-1}(Y_{sc}/X_{sc})$, $\phi = \tan^{-1}(B_y/B_x)$ and $\alpha = \sin^{-1}(\sqrt{1 - Z_{sc}^2}/\sqrt{X_{sc}^2 + Y_{sc}^2})$; these relationships come purely from time-of-flight and geometrical considerations and are the same for ions and electrons. This defines three disturbed regions of solar wind [*Whang*, 1968] as indicated in Figure 1. In these regions, the parallel particle distribution is Maxwellian in the intervals $(-\infty, -\gamma_1 v_{sw})$ in region I, $(\gamma_2 v_{sw}, \infty)$ in region II, and $(-\infty, -\gamma_1 v_{sw}) \cup (\gamma_2 v_{sw}, \infty)$ in region III.

Wind was in region III until roughly 16:40 UT, where the model predicts that the distribution functions have 'notches' of missing particles given by the above relations. Figure 3a shows WAVES/TNR integrated amplitudes in a band, a few kHz wide, centered on f_{pe}, and FFT observations averaged over 0.2 - 6.4 kHz (panel (b)) as well as the bands of missing particles (shown as dark regions in panel (c)); We use thermal speeds $v_{th}^i/v_{sw} = 1/10$ and $v_{th}^e/v_{sw} = 43/10$ [*Ogilvie et al.*, 1996; *Bosqued et al.*, 1996]. After 16:40 UT, the spacecraft enters region II and the distributions are missing particles below the velocity $\gamma_2 v_{sw}$. During the final burst of Langmuir waves starting at 17:35 UT, Wind is moving quickly between regions II and III, as the magnetic field direction fluctuates rapidly.

The effective densities can be calculated from the above distributions and hence a differential density $\delta n = n_i - n_e$. Panel (d) shows the model differential density, δn, that would occur were the plasma unable to provide currents to maintain charge balance. Panels (c) and (d) show that, aside from the umbra and penumbra, this velocity notch affects the electron distribution more strongly; relatively more electrons are depleted from the distribution and the region is left with a net positive charge. In order to avoid the build-up of charge imbalance, the solar wind plasma must produce electric currents along field lines. The resulting current is responsible for the observed ion acoustic waves. Indeed, in the interval from 16:30 to 17:00 UT, the increasing value of δn in panel (d) corresponds to an increasing level of ion acoustic noise in panel (b).

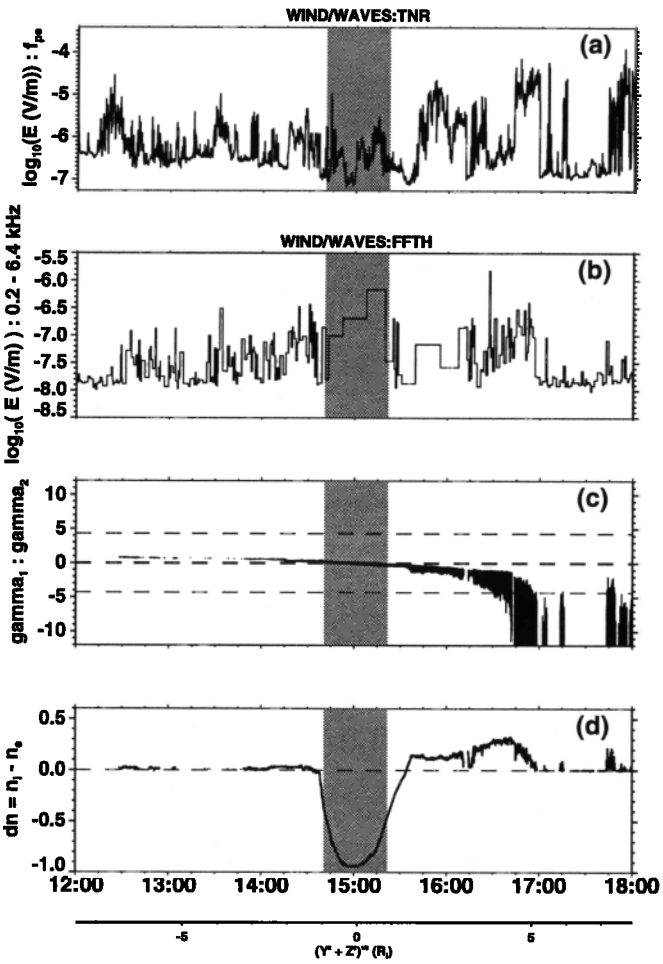

Figure 3. Electric field measurements at the plasma frequency (panel (a)) and averaged over 6.4-0.2 kHz (panel (b)) are shown with the cutoff velocity parameters (panel (c)) and the model density differential δn (panel (d)). The dotted lines in panel (c) show the ion and electron thermal speeds. As the spacecraft passes through the optical wake (vertical bands), the solar wind ion density is depleted. The dark regions in panel (c) correspond to the missing portions of the particle distribution functions. Beyond the optical wake, the effect of velocity cutoff is more important for the electron distribution; regions of positive charge must induce neutralizing currents in the solar wind and these currents can excite waves. During the interval 16:15-17:00 UT, a increase in the model differential density δn corresponds to an increase of ion acoustic noise intensity. The length scale along the bottom axis is the distance from the spacecraft to the $\hat{X}$ axis

The Langmuir and beam mode waves are probably generated by an effective beam distribution similar to the time-of-flight effect in planetary foreshocks [*Filbert and Kellogg*, 1979]. In that scenario, the cutoffs in velocity space provide positive slope features in the electron distribution function and these features are unstable to the generation of Langmuir waves and beam modes. The intense Langmuir waves observations in panel (a) of Figure 3 occur after Wind has moved through the optical wake and is closer to the magnetic field lines tangent to the moon, in agreement with the planetary foreshock scenario.

Conclusion

Ion acoustic waves, Langmuir waves and beam modes are observed when Wind is magnetically connected to the wake of the moon. A generation mechanism is given by the shadowing effect of the moon on solar wind particles. At a given point magnetically connected to the wake, ions and electrons are absent from a certain region of velocity space. The shadowed electron distribution would have inherently unstable features, similar to the time-of-flight effect in the terrestrial electron foreshock which is known to produce Langmuir waves and beam modes.

The differential density calculated from both model distributions implies that the right-hand side of Poisson's equation is finite, and hence a space-charge field must exist. This field will set up a system of currents along connected magnetic field lines to maintain quasineutrality and these currents drive ion acoustic waves.

Wind observations of this ion acoustic noise is thus the first evidence of a current system extending at least 8 R_l into the solar wind on either side of the lunar optical shadow.

Acknowledgments. SDB is funded at QMW by PPARC (UK) grants GR/J88388 and GR/K45791.

References

Bosqued, J. M., et al., Moon-solar wind interaction: First results from the Wind/3DP experiment, Geophys. Res. Lett., 23, 1259, 1996.

Cairns, I. H., Electrostatic wave generation above and below the plasma frequency by electron beams, *Phys. Fluids B*, 1, 204, 1989.

Farrell, W. M., et al., Upstream ULF waves and energetic electrons associated with the lunar wake: Detection of precursor activity, Geophys. Res. Lett., 23, 1271, 1996.

Filbert, P. C. and P. J. Kellogg, Electrostatic noise at the plasma frequency beyond the earth's bow shock, J. Geophys. Res., 84, 1369, 1979.

Kellogg, P. J., et al., Observations of plasma waves during a traversal of the moon's wake, Geophys. Res. Lett., 23, 1267, 1996.

Schubert, G., and B. R. Lichtenstein, Observations of moon-plasma interactions by orbital and surface experiments, *Rev. Geophys. Space Physics*, 12, 592, 1974.

Lyon, E. F., H. S. Bridge, and J. H. Binsack, Explorer 35 plasma measurements in the vicinity of the moon, J. Geophys. Res., 72, 6113, 1967.

Ogilvie, K. M., et al., Observations of the lunar plasma wake from the Wind spacecraft on December 27, 1994, Geophys. Res. Lett., 23, 1255, 1996.

Owen, C. J., et al., The lunar wake at 6.8 R_l: Wind magnetic field observations, Geophys. Res. Lett., 23, 1263, 1996.

Lepping, R. P., et al., The Wind magnetic field investigation, *Space Sci. Rev.*, 71, 207, 1995.

Bougeret, J.-L., et al., WAVES: The radio and plasma wave investigation on the Wind spacecraft, *Space Sci. Rev.*, 71, 231, 1995.

Fuselier, S. A., D. A. Gurnett, and R. J. Fitzenreiter, The downshift of electron plasma oscillations in the electron foreshock region, J. Geophys. Res., 90, 3935, 1985.

Weber, R. R., J. Fainberg, and R. G. Stone, Low frequency radio observations of the solar wind near the moon, Geophys. Res. Lett., 3, 297, 1976.

Whang, Y. C., Interaction of the magnetized solar wind with the moon, *Phys. Fluids*, 11, 969, 1968.

S. D. Bale and C. J. Owen, Astronomy Unit, Queen Mary and Westfield College, Mile End Road, London, E1 4NS, UK (email: S.D.Bale@qmw.ac.uk)

J.-L. Bougeret and R. Manning, DESPA, Observatoire de Paris, Meudon, France 92125

K. Goetz, P. J. Kellogg, and S. J. Monson, School of Physics and Astronomy, University of Minnesota, Minneapolis, MN, 55455 USA

R. P. Lepping, Laboratory for Extraterrestrial Physics, Code 690, NASA/GSFC, Greenbelt, MD 20771 USA

(received January 10, 1997; revised April 2, 1997; accepted April 3, 1997.)